AFRL-RB-WP-TM-2009-3009

SEPARATED TURBULENT SHEAR LAYER MODIFICATION VIA FEEDBACK FLOW CONTROL AND FEEDBACK FLOW CONTROL WITH EXPERIMENT BASED ORDER REDUCTION

Marlyn Y. Andino, Ryan D. Wallace, Ryan F. Schmit, Russell C. Camphouse, James H. Myatt, and Mark N. Glauser

Syracuse University

MARCH 2008
Final Report

AIR FORCE RESEARCH LABORATORY
AIR VEHICLES DIRECTORATE
WRIGHT-PATTERSON AIR FORCE BASE, OH 45433-7542
AIR FORCE MATERIEL COMMAND
UNITED STATES AIR FORCE

NOTICE

Using Government drawings, specifications, or other data included in this document for any purpose other than Government procurement does not in any way obligate the U.S. Government. The fact that the Government formulated or supplied the drawings, specifications, or other data does not license the holder or any other person or corporation; or convey any rights or permission to manufacture, use, or sell any patented invention that may relate to them.

This report was cleared for public release by the Air Force Research Laboratory Wright-Patterson Air Force Base (WPAFB) Public Affairs Office and is available to the general public, including foreign nationals. Copies may be obtained from the Defense Technical Information Center (DTIC) (http://www.dtic.mil).

AFRL-RB-WP-TR-2009-3009 HAS BEEN REVIEWED AND IS APPROVED FOR PUBLICATION IN ACCORDANCE WITH THE ASSIGNED DISTRIBUTION STATEMENT.

//signature//

DR. RYAN SCHMIT

//signature//

DR. MICHAEL STANK, Division Tech Advisor

//signature//

MARVIN GRIDLEY, Acting Branch Chief

This report is published in the interest of scientific and technical information exchange and its publication does not constitute the Government's approval or disapproval of its ideas or findings.

*Disseminated copies will show "//signature//" stamped or typed above the signature blocks.

REPORT DOCUMENTATION PAGE

Form Approved
OMB No. 0704-0188

1. REPORT DATE *(DD-MM-YY)*	2. REPORT TYPE	3. DATES COVERED *(From - To)*
March 2008	Final	25 January 2006 – 31 March 2008

4. TITLE AND SUBTITLE

SEPARATED TURBULENT SHEAR LAYER MODIFICATION VIA FEEDBACK FLOW CONTROL AND FEEDBACK FLOW CONTROL WITH EXPERIMENT BASED ORDER REDUCTION

5a. CONTRACT NUMBER

5b. GRANT NUMBER

FA9550-05-1-0079

5c. PROGRAM ELEMENT NUMBER

0602201

6. AUTHOR(S)

Marlyn Y. Andino, Ryan D. Wallace, James H. Myatt, and Mark N. Glauser (Syracuse University)
Ryan F. Schmit (Aerospace Vehicle Integration and Demonstration Branch (AFRL/RBAI))
Russell C. Camphouse (Control Design and Analysis Branch (AFRL/RBCA))

5d. PROJECT NUMBER

A0C1

5e. TASK NUMBER

5f. WORK UNIT NUMBER

0A

7. PERFORMING ORGANIZATION NAME(S) AND ADDRESS(ES)

Syracuse University
MAME Department
149 Link Hall
Syracuse, NY 13244

Aerospace Vehicle Integration and Demonstration Branch (AFRL/RBAI)
Aeronautical Sciences Division
Air Force Research Laboratory, Air Vehicles Directorate
Wright-Patterson Air Force Base, OH 45433-7542
Air Force Materiel Command, United States Air Force

Control Design and Analysis Branch (AFRL/RBCA)

8. PERFORMING ORGANIZATION REPORT NUMBER

9. SPONSORING/MONITORING AGENCY NAME(S) AND ADDRESS(ES)

Air Force Research Laboratory
Air Vehicles Directorate
Wright-Patterson Air Force Base, OH 45433-7542
Air Force Materiel Command
United States Air Force

10. SPONSORING/MONITORING AGENCY ACRONYM(S)

AFRL/RBAI

11. SPONSORING/MONITORING AGENCY REPORT NUMBER(S)

AFRL-RB-WP-TM-2009-3009

12. DISTRIBUTION/AVAILABILITY STATEMENT

Approved for public release; distribution unlimited.

13. SUPPLEMENTARY NOTES

PAO Case Numbers: WPAF 07-0303, WPAFB 07-0304, and WPAFB 07-0496; clearance date 01 November 2007. Report contains color.

14. ABSTRACT

Losses in the performance and effectiveness of optical systems are caused by turbulence. In particular, separated turbulent flow phenomena are present in several aero-optics applications. In an effort to reduce the adverse effects of turbulence, we are exploring the use of both open and closed-loop flow control. A series of experiments were performed in Syracuse University and Wright-Patterson Air Force Base (WPAFB) facilities using two test models, a quarter- and half-scale, respectively. The 3D turrets contained an actuation system that consists of 11 to 17 synthetic jets placed upstream from the leading edge of the aperture. Different actuation cases were tested to then evaluate the effects of the flow control over the aperture area and their control authority. Simultaneous surface pressure and particle image velocimetry (PIV) measurements in the separated region were performed, both with and without flow control. The PIV results for the Syracuse test suggest that with the open-loop control the separation zone above the aperture is reduced spatially and the mean square velocity fluctuations reduced in amplitude by 15 to 20 percent. Pressure results from the closed loop test at WPAFB present a 20 percent reduction in the amplitude when compared to the open loop results.

15. SUBJECT TERMS

Closed loop feedback flow control, Particle Image Velocimetry separated turbulence flows

16. SECURITY CLASSIFICATION OF:			17. LIMITATION OF ABSTRACT:	18. NUMBER OF PAGES	19a. NAME OF RESPONSIBLE PERSON (Monitor)
a. REPORT	b. ABSTRACT	c. THIS PAGE			Ryan F. Schmit
Unclassified	Unclassified	Unclassified	SAR	20	19b. TELEPHONE NUMBER *(Include Area Code)* 937-904-8177

Standard Form 298 (Rev. 8-98)
Prescribed by ANSI Std. Z39-18

Table of Contents

Section **Page**

Losses in the performance and effectiveness of optical systems are caused by turbulence. In particular, separated turbulent flow phenomena is present in several aero-optics applications. In an effort to reduce the adverse effects of turbulence, we are exploring the use of both open and closed-loop flow control. A series of experiments were performed in Syracuse University and Wright-Patterson Air Force Base facilities using two test models, a quarter- and half-scale, respectively. The 3D turrets contained an actuation system that consists of 11 - 17 synthetic jets placed upstream from the leading edge of the aperture. Different actuation cases were tested to then evaluate the effects of the flow control over the aperture area and their control authority. Simultaneous surface pressure and PIV velocity measurements in the separated region were performed, both with and without flow control. The PIV results for the Syracuse test suggest that with the open-loop control the separation zone above the aperture is reduced spatially and the mean square velocity fluctuations reduced in amplitude by 15 - 20 percent. Pressure results from the closed loop test at WP-AFB present a 20 percent reduction in the amplitude when compare to the open loop results.

I. Introduction

Turbulence degrades the performance of airborne optical systems[10,9,.2] Aero-optical effects are among the factors taken into account to determine the effectiveness of these systems. The light beam is particularly affected as it passes through: separated flow, boundary and shear layers, and inviscid flow.[6] Passive flow control devices for these applications have been tested[8] and have shown an improvement of the optical environment. A possible second method of cleaning up the flow is to utilize active flow control. Previous research done by Glauser *et al.* (2004) and Ausseur *et al.* (2006), using active flow control devices, demonstrated the use of low dimensional tools for the development of real-time closed loop control, using actuators to control the flow over a NACA-4412 airfoil. In this effort to reduce the laser light diffusion similar methods of analysis and control schemes were implemented to positively affect the flow over the optical device.

The particular geometry of interest is a half hemisphere turret with a flat aperture where the optical device would be located. Flow around the 3D turret is highly complex especially at higher Mach numbers. An understanding of the flow physics around this geometry is needed in order to be able to design an effective control design. The area over the optical device is of the most concern. Experiments were performed on the flow over the 3D turrets at a Mach number of 0.1 and 0.3 corresponding to Reynolds numbers of $600,000$ and $2,000,000$ respectfully, based on the diameter and free stream velocity. The turrets were design with an actuation system consisting of synthetic jets created by pairs of piezoelectric disks actuated in phase. The actuation system was placed upstream from the leading edge of the aperture. Various actuation cases were tested and evaluated to understand the effects of the flow control over the aperture area.

Our main objective is to develop a robust, real-time closed loop flow control system capable of improving the aero-optical path of a laser beam. A large database of velocity flow field data along with simultaneously sampled surface pressure measurements was obtained. Using this large data set, the flow characteristics and properties are able to be analyzed and understood. Building upon the flow physics, mathematical tools such as, Proper Orthogonal Decomposition, *POD*, and Modified Linear Stochastic Measurements, *mLSM*, will be further applied to reconstruct the flow and also used to develop a proportional feedback flow control model.

II. Experimental setup

A. SU Wind Tunnel

A quarter-scale turret has been constructed and tested in a subsonic wind tunnel facility at Syracuse University. The Gottingen-type, closed, recirculating tunnel is a horizontal configuration with continuously variable speeds of less than 4 m/s to above 60 m/s. Tests with the turret were performed at 30 m/s (Mach number of 0.1 and Reynolds number based on turret diameter of $300,000$). The test section is constructed of optical plexiglass with dimensions of 24 $in.$ (w) $\times$ 24 in (h) $\times$ 96 $in(l)$. The turret is a six-inch diameter hemisphere mounted on a cylindrical base approximately four inches in height. Figure 1(a) contains a computer-aided design rendering of the test article.

The turret is mounted on a splitter or mounting plate 15 inches long, 12 inches wide, and 0.5 inches thick. The mounting plate facilitates variable−angle−of−attack tests, using a motor-driven pitching system that has been constructed for the SU wind tunnel. The smaller turret's circular, optical aperture is flat, has a radius of 1.4 inches, and is located at the apex of the hemisphere. The aperture was set at a boresight angle of 120 degrees for all the studied cases. An array of actuators located upstream of the aperture consists of 11 synthetic jets: 11 cavities housing 22 ceramic piezo-electric diaphragms. Each cavity houses two diaphragms in order to provide a broad range of actuator input. The diaphragms are 1.07 inches in diameter with a resonant frequency of 2.6 kHz. Open-loop tests recorded jet velocities of up to 50 m/s at 1 mm above the cavity opening. The diaphragms operate at a resonant frequency of 2.6 kHz.

Measurements are based on two sets of surface-mounted pressure transducers: 15 evenly-spaced at the aperture and 15 downstream of the aperture. Actuators and pressure transducers are configured in a modular fashion to enable rearrangement when required. The Acoustic ICP sensors have a measurement range of 181 dB, a resolution of 77 dB, a sensitivity of 1500 mV/kPa, a resonant frequency of greater than 13 kHz, and a low-frequency response of 5 Hz. Particle Image Velocimetry, *(PIV)*, measurements have been taken in five planes equally spaced over the top of the turret. In the SU facility, a DANTEC PIV System measures two components of velocity in the planes. Velocity measurements are sampled at a rate of 4 kHz using a DANTEC FLOWMAP system. Pressure transducer are sampled at 10 kHz using a NATIONAL INSTRUMENTS PXI-based 800 MHz signal conditioner with dedicated 24 bit high-resolution A/D converters and anti-aliasing filter.

The PXI-A/D system has an external trigger to temporally link pressure measurements and PIV velocity measurements. With each laser pulse, corresponding to one snapshot of the flow, a signal is sent from the PIV processing unit to the PXI, and a marker is inserted in the continuous stream of pressure data. The phase-aligned information (velocity field above the turret and surface pressure on the turret) is input to a measurement-based estimator. The PIV system is composed of CCD cameras (1280 $\times$ 1024 pixels, each) and mounts, double pulsed NEWWAVE RESEARCH 200 mJ Nd:YAG lasers, light sheet optics and a post-processing unit. Figure 1(b) contains a schematic of the test section, turret, and PIV measurement system—mounted on a pitching system to facilitate variable angle of attack runs. A TSI olive oil based seeder is used to produce spherical liquid particles with diameters between 1 and 5 μm, which follow the fluctuations in the fully turbulent flow. The seeding is introduced directly downstream of the turret and allowed to circulate through the tunnel before measurements begin.

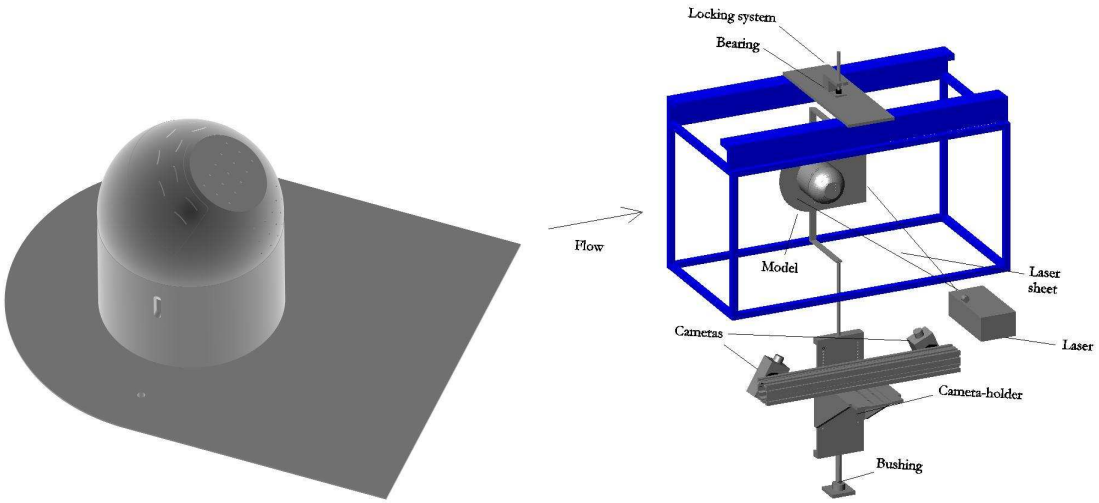

(a) Test article.

(b) Wind tunnel test setup overall view.

Figure 1. The SU test configuration.

B. SARL Wind tunnel

Figure 2. Subsonic Aerodynamic Research Laboratory, *SARL*, at Wright-Patterson,OH

The Subsonic Aerodynamic Research Laboratory, *SARL*, wind tunnel at Wright Patterson Air Force Base is an open loop wind tunnel with a test section that is 7 feet wide by 10 feet high. The wind tunnel has a capacity to generate a flow between Mach number 0.1 to Mach number 0.5. Wind tunnel tests were ran at a Mach number 0.3 to 0.4 corresponding to Reynolds number $2,000,000$ to $2,800,000$ respectively, based on diameter and free stream velocity. SARL's test section is equipped with plexi-glass windows all around the test section, as seen in Figure 2, which made it possible to conduct PIV measurements. A tent was set up covering the test section to block the ambient light from interfering with the PIV measurements and allow for the cooling of the instrumentation.

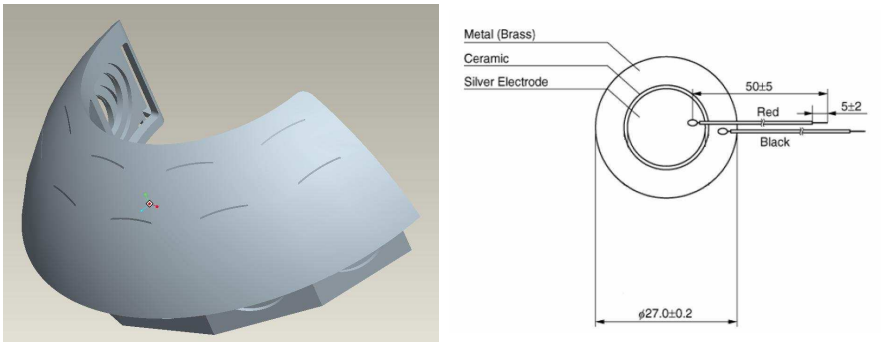

(a) (b)

Figure 3. (a) Actuation bank located by the leading edge of cylindrical turret and (b) Ceramic piezo-electric actuator disk of $1.07\ in$**.**

The turret consists of a hemisphere and a cylindrical base as shown in figure 4(a). The hemisphere is 12 inches in diameter with a 5 inches flat aperture at the top of the hemisphere. The aperture is set to have a boresight angle of 120 degrees, with respect to the incoming flow, facing downstream. On the upstream surface of the turret is an array of 17 synthetic jets. Each synthetic jet utilizes two ceramic piezo-electric diaphragms sealed into a cavity with only a thin slot to pulse the air. The actuators, as shown in figure 3, have a diameter of 1.07 inches with a resonant frequency of 2.6 kHz. The diaphragms operate at a resonant frequency of 2.6 kHz. At its optimum frequency the synthetic jets were able to produce velocities of 50 m/s.

A 5 inch cylindrical base is used to mount and adjust the angle of attack of the hemisphere. Attached underneath to the turret is a splitter plate that is 3 feet wide by 5 feet long.

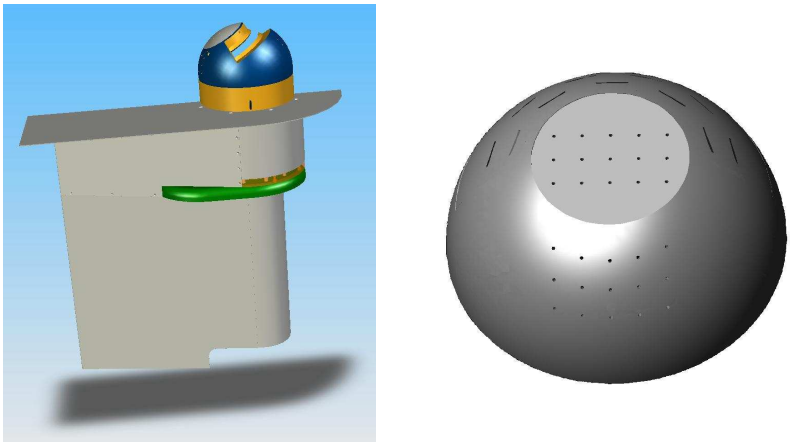

(a) SARL's turret configuration

(b) Pressure sensors distribution over the hemisphere

Figure 4. SARL test article setup.

Uniformly spaced surface mounted transducers on the hemisphere measured the pressure along the surface of the turret at two main locations: 16 transducers on the aperture and 15 transducers downstream of the aperture, as seen in Figure 4(b). The Acoustic ICP sensors have a measurement range of 181 dB, a resolution of 77 dB, a sensitivity of 1500 mV/kPa, a resonant frequency of greater than 13 kHz, and a low-frequency response of 5 Hz.

Pressure measurements were recorded with a NATIONAL INSTRUMENTS PXI-based 800 MHz signal conditioner with dedicated 24 bit high-resolution A/D converters and anti-aliasing filters. The experiments at SARL consisted of simultaneously sampling of the surface pressure on the turret and the velocity field around the turret.

Velocity measurements in the free stream and wake of the turret were obtained by utilizing a DANTEC FLOWMAP Particle Image Velocimetry, *(PIV)*, system. The velocity field was taken at seven separate planes. All the planes were parallel to each column of pressure transducers which were approximately one inch apart. PIV images were sampled at a rate of 4 Hz and 1000 statistically independent samples were taken for each test case. The PXI system simultaneously recorded the PIV pulse and the pressure measurements linking both the velocity and pressure data at 8.5 kHz. These snapshots will be use to construct the velocity correlation tensor and low-dimensional POD-based model as described in Glauser et al (2004) and Pinier et al (2007).

The PIV system is composed of a dual pulse laser and two CCD cameras. The dual pulse laser is a NEWWAVE RESEARCH 200 mJ Nd:YAG with light sheet optics. The cameras contain a CCD chip and have 1280 $\times$ 1024 pixels each. The solid particle Talc, is used to seed the flow. Individual particle size varies from 1 m to 10 m. Talc was seeded at a significant distance upstream of the turret allowing the seed to diffuse and form a homogeneous particle flow.

III. POD and mLSM low-dimensional techniques

A. Proper Orthogonal Decomposition

Proposed by Lumley in 1967 as a technique to study the coherent structures in turbulent flows. POD extracts the most energetic features in the flow allowing us to have a large percentage of the system dynamics in

a small number of modes. We use this to decompose the velocity field. This results on a finite number of empirical eigenfunctions that form a discrete set of uncorrelated orthogonal functions given by the following eigenvalue problem:

$$\int R_{ij}(\vec{x},\vec{x}')\phi_j^{(n)}(\vec{x}'),d\vec{x}' = \lambda^{(n)}\phi_i(\vec{x}). \tag{1}$$

where $R_{ij}(\overrightarrow{x},\overrightarrow{x}')$ is the ensemble averaged two-point spatial velocity correlation tensor, defined as:

$$R_{ij}(\vec{x},\vec{x}') = \overline{u_i(\vec{x},t_o)u_j(\vec{x}',t_o)} \tag{2}$$

where t_o is a given snapshot time. We then can extract the time dependent expansion coefficients describing the flow, by projecting the velocities onto the eigenfunctions, as follows:

$$a_n(t_o) = \int_D u_i(\vec{x},t_o)\phi_i^{(n)*}(\vec{x})\,d\vec{x} \tag{3}$$

where $u_i(\vec{x},t_o)$ is the velocity field at a given snapshot time.

The eigenfunctions of equation 1 called empirical eigenfunctions since they are derived from the ensemble of the observations. Now we can reconstruct original velocity field, u_i, by projecting $a_n(t)$ on the eigenfunctions:

$$u_i(\vec{x},t_o) = \sum_{n=1}^{N} a_n(t_o)\phi_i^{(n)}(\vec{x}) \tag{4}$$

where N is the number of modes which we wish to use to reconstruct the velocity field. If N is ∞ the velocity field is completely reconstructed. We use the time dependent information provided by equation 4 to develop the low-dimensional descriptions of the flow when N is a finite number. The POD method allows us to have an accurate representation of the flow physics in a low dimensional model.

B. modified Linear Stochastic Measurement

The Linear Stochastic Estimation was proposed by Adrian in 1975. He recognize that the statistical information in the correlation tensor from POD could be combined with instantaneous data to estimate the flow field containing a "conditional eddy".

Bonnet *et al.* (1994) expanded on the work of Adrian (1975) to form the complementary technique which combines POD and LSE to obtain time dependent POD expansion coefficients from instantaneous velocity data on course hot wire grids.

Glauser (2004) further expanded these methods and demonstrated how instantaneous wall pressure measurements could be used to construct an accurate representation of the instantaneous velocity field from wall pressure alone (i.e., the modified complementary technique or mLSE, now termed mLSM). In this study we will use the mLSM method to compute the POD velocity coefficients above the turret using discrete pressure measurements taken on its surface. The instantaneous wall pressure is used in equation 5,

$$\tilde{a}_n(t) = \langle a_n(t)|p(t)\rangle \tag{5}$$

to obtain $\tilde{a}_n(t)$ the estimate of the random POD coefficient that describes the velocity field over $\overrightarrow{x}$ given the instantaneous surface pressures, $p_i(t)$. The estimated random coefficients for each POD mode can be described as a series expansion using the instantaneous surface pressures available at i positions on the airfoil surface:

$$\tilde{a}_n(t) = B_{n1}p_1(t) + B_{n2}p_2(t) + \cdots + B_{nq}p_q(t). \tag{6}$$

Truncating this expression to include only the linear term (plus the error associated with neglecting the higher order terms) we obtain:

$$\tilde{a}_n(t) = B_{ni}p_i(t) + O[p_i^2(t)]. \tag{7}$$

The coefficients are considered to be the conditional structures of the flow, and they effectively describe a certain percentage of the energy contained in a certain spatial POD mode. The elements of B_{ni} are chosen to minimize the mean square error, $e_{\tilde{a}_n} = \overline{[\tilde{a}_n(t) - a_n(t)]^2}$ by requiring that $\frac{\partial e_{\tilde{a}_n}}{\partial B_{ni}} = \frac{\partial \overline{[B_{ni}p_i(t) - a_n(t)]^2}}{\partial B_{ni}} = 0$. The solution to the minimization problem of equation 7 is a linear system of equations, which can be written in matrix form as:

$$\begin{bmatrix} \langle p_1^2 \rangle & \langle p_1 p_2 \rangle & \cdots & \langle p_1 p_q \rangle \\ \langle p_2 p_1 \rangle & \langle p_2^2 \rangle & \cdots & \langle p_2 p_q \rangle \\ \vdots & \vdots & \ddots & \vdots \\ \langle p_q p_1 \rangle & \langle p_q p_2 \rangle & \cdots & \langle p_q^2 \rangle \end{bmatrix} \begin{bmatrix} B_{n1} \\ B_{n2} \\ \vdots \\ B_{nq} \end{bmatrix} = \begin{bmatrix} \langle a_n p_1 \rangle \\ \langle a_n p_2 \rangle \\ \vdots \\ \langle a_n p_q \rangle \end{bmatrix}$$

The elements B_{ni} are then substituted into equation 7 to estimate the random POD coefficient for each instantaneous pressure measurement. These coefficients when combined with the POD eigenfunctions provide an estimate of the instantaneous velocity field, $u_i(t)$ from application of equation 4. This method has been used[3,7] for flow control studies to provide the state of the flow from wall pressure only.

IV. Results and Future Work

A. SU turret

For this test model, three cases were studied for open loop: baseline and two actuated cases. In the first actuated case, the diaphragms were driven at a dimensionless frequency, f^+, of 1 and in the second case the actuation frequency was set at the natural frequency of the piezo-electric diaphragms. A previous test to calibrate each jet was done were the exit velocity was quantify for a range of frequency no greater than the resonant frequency of each diaphragm. In this process an amplitude was selected to give us an output voltage smaller than the peak-to-peak voltage limit for the diaphragm. The next step was to select the frequencies that would provide us with an exit velocity of 50 m/s. This parameters provided us with a momentum coefficient of 0.009. The center plane was selected as the study plane for the results presented here.

By examining the mean square values for these cases, presented in figure 5, it seems that the actuation in both cases reduced the thickness of the shear layer. A reduction of $10 - 20\%$ is perceived, when we compare the turbulence strength levels of the baseline case with the two actuated cases. Similar results are found in the Reynolds shear stress, shown in figure 6.

B. SARL turret

In the process of developing a robust closed feedback loop system, a database of various actuated open loop cases were tested. The databases consisted of simultaneously sampled surface pressure on the turret and the velocity field around the turret. The first case within the database is the baseline case of no control. Open loop control was then applied to the flow by actuating the synthetic jets. The database of this open loop control study, includes actuated cases such as: a sine wave, a range of various modulated sine waves with different non-dimensional frequencies, and a range of various modulated square waves with different non-dimensional frequencies. For each case, 1000 statistically independent measurements were taken in seven spanwise planes over the turret. We are currently analyzing velocity measurements.

In figure 7, we show the pressure signature for a sensor that is located in the center plane, about an 1.5 inches from the leading edge of the aperture. A small reduction in the amplitude of the pressure for the case of modulated square wave is shown in figure 7(d). Further analysis is expected to be done to examine the length scale changes as a function of the excitation input.

Proper orthogonal decomposition,[11] *POD*, based on the snapshot method[13] was applied to surface pressure data obtained via transducers over the aperture. Pressure data over the aperture was collected for the baseline flow field as well as 12 open-loop actuation cases. Actuated cases were comprised of periodic and pulsed-modulated input signals of varying frequency. An ensemble of $2,000$ snapshots of the baseline pressure field and 300 snapshots from each actuated case were taken, resulting in a total of $5,900$ snapshots. From these, low-dimensional bases for the pressure field over the aperture were constructed using three different methods.

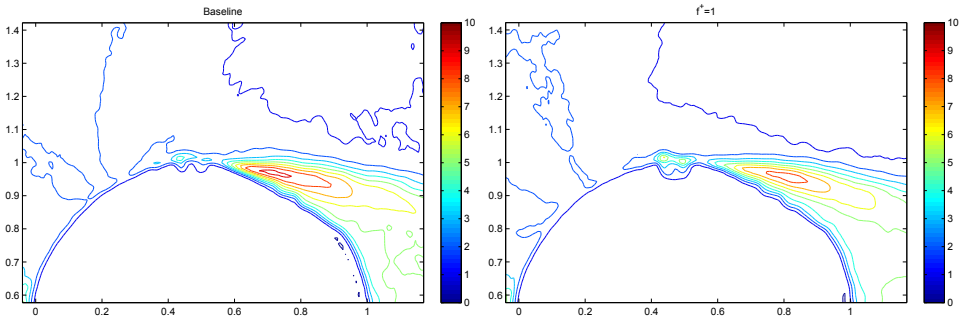

(a) Baseline (b) Actuation, $f^+ = 1$

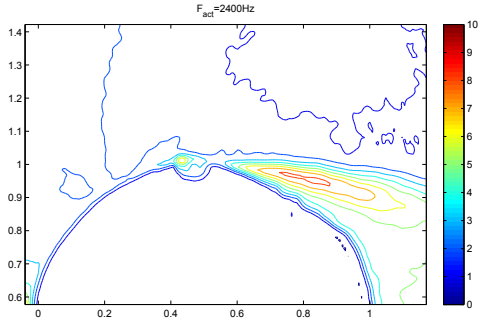

(c) Actuation, $f_{act} = 2600\ Hz$

Figure 5. Mean square for U-component of the velocity field.

In the first method, only baseline data was used to construct the POD basis. The resulting expansion of the pressure field over the aperture in terms of the baseline POD basis is of the form

$$p(t,x,y) = \sum_{m=1}^{M_B} a_m(t)\varphi_m(x,y) \tag{8}$$

where M_B denotes the number of the baseline modes used in the expansion and $a_m(t)$ is the temporal coefficient for the mth baseline mode $\varphi_m(x,y)$.

For the second method, baseline and actuated cases were lumped together, resulting in an ensemble containing both baseline and actuated pressure data. Snapshot POD was applied to the overall lumped ensemble to generate a basis spanning both the baseline and the actuated pressure fields. The resulting pressure field expansion is of the form

$$p(t,x,y) = \sum_{m=1}^{M_L} b_m(t)\phi_m(x,y) \tag{9}$$

where M_L denotes the number of lumped POD modes used in the expansion and $b_m(t)$ is the temporal coefficient for the mth lumped mode $\phi_m(x,y)$.

Finally, in the third case, each actuated snapshot was decomposed into a baseline component and an orthogonal component due to actuation. POD was applied separately to the baseline and actuated pressure data resulting from this decomposition to obtain a split-POD[5] basis. The resulting pressure field expansion is of the form

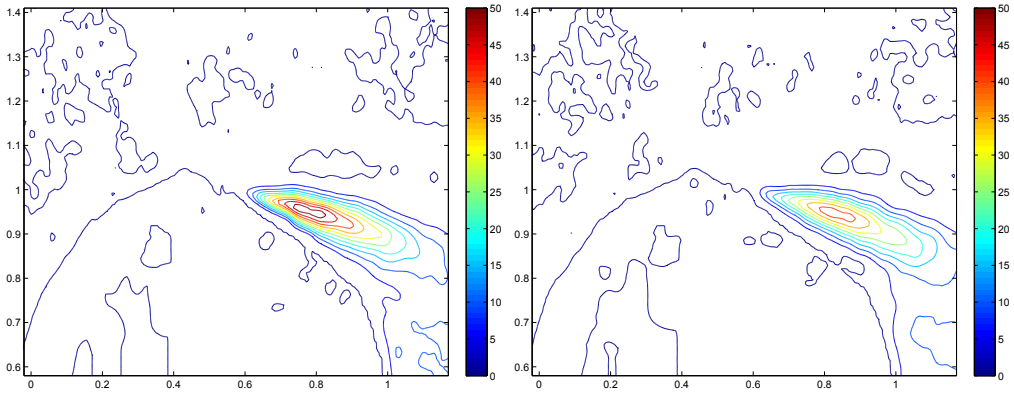

(a) Baseline

(b) Actuation ON, $f^+ = 1$

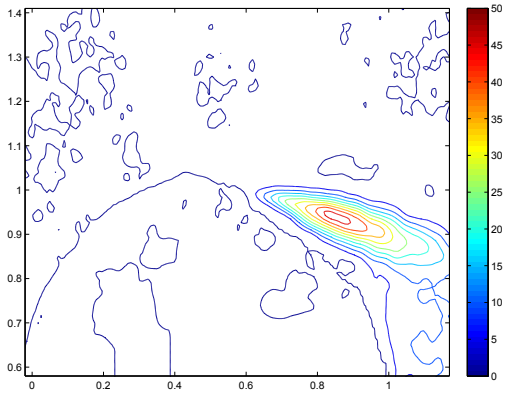

(c) Actuation ON, $f_{act} = 2400\ Hz$

Figure 6. Reynolds shear stress at the centerline.

$$p(t,x,y) \;=\; \sum_{m=1}^{M_B} a_m(t)\varphi_m(x,y) + \sum_{n=1}^{M_A} c_n(t)\xi_n(x,y) \tag{10}$$

Note that in equation 10, the baseline pressure field is expanded and in equation 8. For the second sum in equation 10, actuated pressure field information is represented in terms of the actuated POD basis resulting from snapshot decomposition. In equation 10, M_A is the number of actuator modes used in the expansion and $c_n(t)$ is the nth temporal coefficient, corresponding to the actuator mode $\xi_n(x,y)$.

A simple feedback controller was implemented in the wind tunnel for each of the three cases above. The control objective was to reduce or eliminate the large fluctuations in the pressure over the aperture. The controller was of the form

$$u(t) \;=\; -K\left[\sum_{i=1}^{M} a_i(t)\right] \sin\Big(2\pi f_0(t-t_0)\Big) \tag{11}$$

In equation 11, K is a constant feedback gain, $\{a_i\}_{i=1}^{M}$ are the POD temporal coefficients, f_0 is the characteristic frequency of the synthetics jet actuators, and t_0 is a phase shift to compensate for the time

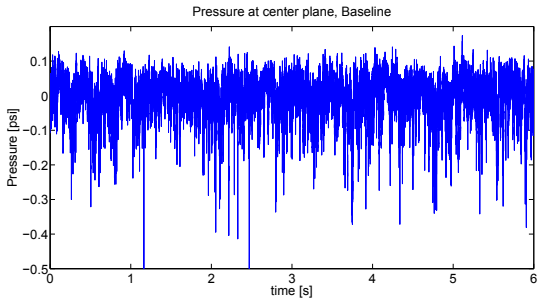

(a)

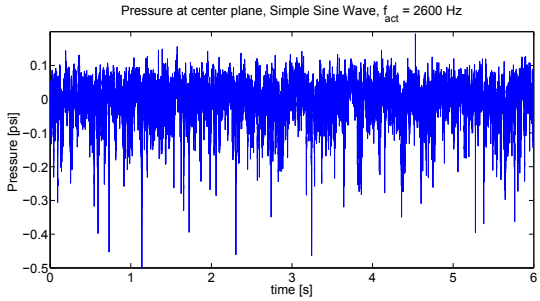

(b)

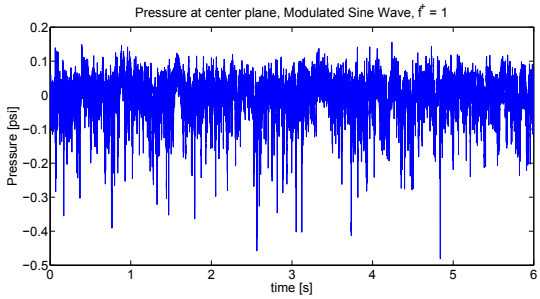

(c)

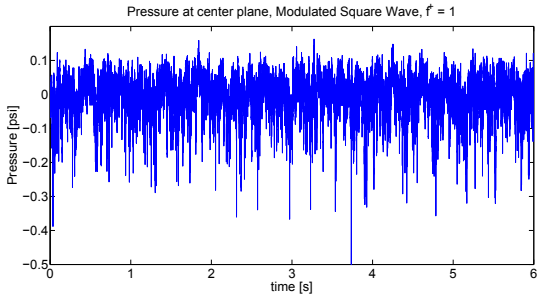

(d)

Figure 7. Pressure signal at $M = 0.3$: (a) Baseline, (b) $f_o = 2600\ Hz$, (c) modulated sine wave with $f^+ = 1$, and (d) modulated square wave with $f^+ = 1$, 50% duty cycle.

delay between the actuators and sensors. The temporal coefficients in equation 11 were determine in real-time during the experiment by projecting sensor pressure data onto the baseline, lumped, or split-POD cases. The number of modes chosen in equation 11 corresponds to the number of modes necessary for each of the basis construction methods outlined above. In particular, $M = M_B$ for the expansion in equation 8. For the expansion in equation 9, $M = M_L$. Finally, $M = M_B + M_A$ for the expression in equation 10. To determine the impact of additional modes on control effectiveness, controllers were constructed using only one mode in expansions 8-10, i.e. $M_B = M_L = M_A = 1$, as well as the number of modes necessary to capture 99%of the energy from the pressure data of the baseline and the three different POD methods. Figure 8 shows the baseline and the three POD methods using the modes to capture 99% of the energy.

As seen in figures 8(b)-8(d), preliminary results from the pressure data shows that there is a reduction in the mean square value as compared to figure 8(a). Closed loop control clearly provides a positive effect on the wake of the turret. It can be concluded that the Split POD, shown in figure 8(d), was the most effective input. These results indicate that there is enough control authority for this configuration from the fluids point of view. Further analysis of the aero-optic field will evaluate the efficiency of the control system in reducing the adverse aero-optic effects caused by the separated flow.

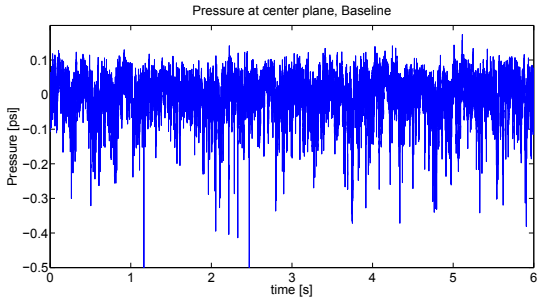

(a)

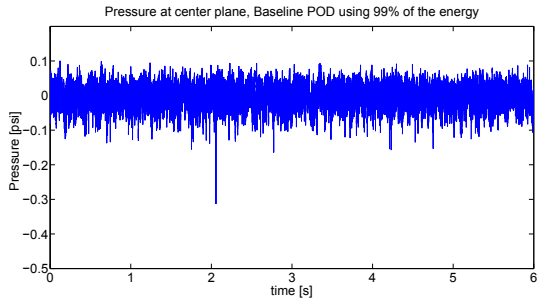

(b)

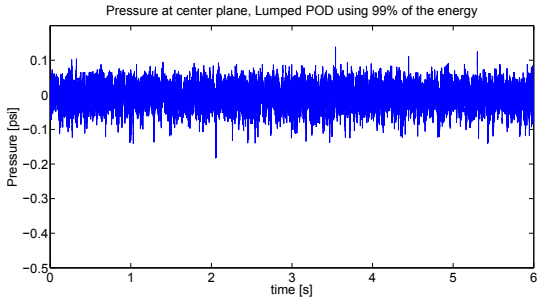

(c)

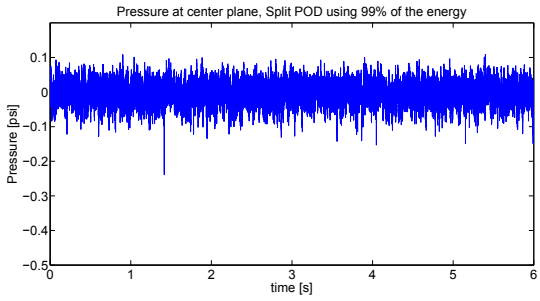

(d)

Figure 8. Pressure signal at $M = 0.3$: (a) Baseline, (b) Baseline POD , (c) Lumped POD, and (d) Split POD.

References

[1]Adrian, R.J. (1975). On the role of condiotional averages in turbulence theory, *In Proc. 4th Biennal Symp. on Turbulence in Liquids*

[2]Arunajatesan, S., Sinha,N., and Kannepalli, C., "Analysis of lenght scale effects in distortions of laser beams propagating through turbulents flows", *37th AIAA Plasmadynamics and Lasers Conference - AIAA 2006-3071*, San Francisco, CA, June 5-8, 2006.

[3]Ausseur, J., Pinier, J., Glauser, M., Higuchi, H.,and Carlson, H., "Experimental development of a reduced-order model for flow separation control", *44th AIAA Aerospace Sciences and Exhibit - AIAA 2006-1251*, Reno, Nevada, January 9-12, 2006.

[4]Bonnet, J.P., Cole, D.R., Delville, Glasuer,M.N., Ukeiley, L.S. (1994). Stochastic estimation and proper orthogonal decomposition: Complimentary techniques for idntifying structures. *Experiments in Fluids*, 17, pp 307-314.

[5]Camphouse, R.C., Myatt, J.H., Schmit, R.F., Snyder, B.L., Glauser, M.N., Ausseur, J.M., Andino, M.Y., and Wallace, R.D., "A snapshot decomposition method for reduced order modeling and boundary feedback control", 4*th AIAA Flow Control Conference*, Seattle, Washington, June 23-26, 2008.

[6]Gilbert, K.G. and Otten, L.J. (Eds.). (1982). Aero-optical phenomena. *Progress in astronautics and aeronautics*, Vol. 40, AIAA, New York.

[7]Glauser, M.N., Higuchi, H., Ausseur, J., and Pinier, J.,"Feedback control of separated flows.", 2*nd AIAA Flow Control Conference - AIAA 2004-2521*, Portland, OR, June 28-July 1, 2004.

[8]Gordeyev, S., Jumper, E.J., Ng, T., and Cain, A.B., "The optical environment of a cylindrical turret with a flat window and the impact of passive control devices", *36th AIAA Plasmadynamics and Lasers Conference - AIAA2005-4657*, Toronto, Canada, June 6-9, 2005.

[9]Gordeyev, S., Hayden, T., and Jumper, E., "Aero-optical and flow measurements over a flat-windowed turret", *AIAA Journal*, Vol. 45, No. 2, 2007.

[10]Jumper, E.J., and Fitzgerald, E.J., "Recent advances in aero-optics", *Progress in aerospace sciences*, Vol. 37, No. 3, 2001, pp. 229-339.

[11]Lumley, J.L. (1967). The structure of inhomogeneous turbulence. In Yaglom, A.M. and Tatarski, V.I., editors, *Atmospheric turbulence and radio wave propagation*, pp. 166-178. Nauka, Moscow.

[12]Pinier, J.T., Ausseur, J.M., Glauser, M.N., and Higuchi, H., Proportional closed-loop feedback control of flow separation, *AIAA Journal*, Vol.45, No.1, 2007, pp. 181-190.

[13]Sirovich, L., "Turbulence and the dynamics of coherent structures, Parts I-III", *Quarterly of applied mathematics*, 45, Brown University, Rhode Island, 1987, pp. 561-590.